

Ca²⁺ release via IP₃ receptors shapes the cytosolic Ca²⁺ transient for hypertrophic signalling in ventricular cardiomyocytes

Hilary Hunt¹, Agnė Tilūnaitė¹, Greg Bass¹, Christian Soeller², H. Llewelyn Roderick³, Vijay Rajagopal^{*†4}, and Edmund J. Crampin^{*†1,5}

¹Systems Biology Laboratory, School of Mathematics and Statistics and Melbourne School of Engineering, University of Melbourne, Australia

²Living Systems Institute, University of Exeter, UK

³Laboratory of Experimental Cardiology, Department of Cardiovascular Sciences, KU Leuven, Belgium

⁴Cell Structure and Mechanobiology Group, Department of Biomedical Engineering, Melbourne School of Engineering, University of Melbourne, Australia

⁵ARC Centre of Excellence in Convergent Bio-Nano Science and Technology, School of Chemical and Biomedical Engineering, University of Melbourne, Australia

*Correspondence: vijay.rajagopal@unimelb.edu.au; edmund.crampin@unimelb.edu.au

ABSTRACT Calcium (Ca²⁺) plays a central role in mediating both contractile function and hypertrophic signalling in ventricular cardiomyocytes. L-type Ca²⁺ channels trigger release of Ca²⁺ from ryanodine receptors (RyRs) for cellular contraction, while signalling downstream of Gq coupled receptors stimulates Ca²⁺ release via inositol 1,4,5-trisphosphate receptors (IP₃Rs), engaging hypertrophic signalling pathways. Modulation of the amplitude, duration, and duty cycle of the cytosolic Ca²⁺ contraction signal, and spatial localisation, have all been proposed to encode this hypertrophic signal. Given current knowledge of IP₃Rs, we develop a model describing the effect of functional interaction (cross-talk) between RyR and IP₃R channels on the Ca²⁺ transient, and examine the sensitivity of the Ca²⁺ transient shape to properties of IP₃R activation. A key result of our study is that IP₃R activation increases Ca²⁺ transient duration for a broad range of IP₃R properties, but the effect of IP₃R activation on Ca²⁺ transient amplitude is dependent on IP₃ concentration. Furthermore we demonstrate that IP₃-mediated Ca²⁺ release in the cytosol increases the duty cycle of the Ca²⁺ transient, the fraction of the cycle for which [Ca²⁺] is elevated, across a broad range of parameter values and IP₃ concentrations. When coupled to a model of downstream transcription factor (NFAT) activation, we demonstrate that there is a high correspondence between the Ca²⁺ transient duty cycle and the proportion of activated NFAT in the nucleus. These findings suggest increased cytosolic Ca²⁺ duty cycle as a plausible mechanism for IP₃-dependent hypertrophic signalling via Ca²⁺-sensitive transcription factors such as NFAT in ventricular cardiomyocytes.

SIGNIFICANCE Many studies have identified a role for IP₃R-mediated Ca²⁺ signalling in cardiac hypertrophy, however the mechanism by which this signal is communicated within the cardiomyocyte remains unclear. We present a mathematical model of functional interactions between RyR and IP₃R channels. We show that IP₃-mediated Ca²⁺ release is capable of providing a modest increase to the duty cycle of the calcium signal, which has been shown experimentally to lead to NFAT activation, and hence hypertrophic signalling. Through a parameter sensitivity analysis we demonstrate that the duty cycle is increased with IP₃ over a broad parameter regime, indicating that this mechanism is robust, and we show that an increase in Ca²⁺ duty cycle increases nuclear NFAT activation. These findings suggest a plausible mechanism for IP₃R-dependent hypertrophic signalling in cardiomyocytes.

INTRODUCTION

Calcium is a universal second messenger that plays a role in controlling many cellular processes across a wide variety of cell types; ranging from fertilisation, cell contraction, and cell growth, to cell death (1, 2). Precisely how Ca²⁺ fulfills each of these

[†]These authors contributed equally to the supervision of this work.

roles while also ensuring signal specificity remains unclear in many cases. Ca^{2+} can be used to transmit signals in a variety of ways. Signal localisation, and amplitude and frequency modulation have been widely explored (3–5), however, mechanisms for information encoding in the cumulative signal (i.e. area under the curve (AUC), proportional-integral-derivative (PID) controller, or duty cycle (DC)) have also been proposed (6–8). Determining which method of information encoding is relevant to a specific signalling pathway requires determining what type of signal encoding the system is capable of, and whether the downstream effector of the signal is capable of temporal signal integration, high or low pass filtering, or threshold filtering.

In cardiac myocytes, discrete encoding of multiple Ca^{2+} -mediated signals is particularly pertinent because of the essential and continuous role Ca^{2+} plays in excitation-contraction coupling (ECC). Of particular significance is the involvement of Ca^{2+} in hypertrophic growth signaling. How Ca^{2+} can communicate a signal in the hypertrophic signalling pathway concurrent with the cytosolic Ca^{2+} fluxes that drive cardiac muscle contraction is still largely unresolved (9, 10). Understanding this mechanism is important as pathological hypertrophic remodelling is a precursor of heart failure and a common final pathway of cardiovascular diseases including hypertension and coronary disease (11–13).

During each heartbeat, on depolarisation of the membrane Ca^{2+} enters the cell via L-type Ca^{2+} channels (LTCC), triggering larger Ca^{2+} release from the sarcoplasmic reticulum (SR) via ryanodine receptors (RyRs), which then induces contraction. The activation of Ca^{2+} release via RyRs by the Ca^{2+} arising via LTCCs is known as calcium-induced calcium release (CICR), and results in a 10-fold increase in cytosolic Ca^{2+} concentration (relative to resting Ca^{2+} concentration of ~ 100 nM). Sarco-endoplasmic reticulum Ca^{2+} pumps (SERCA) and other Ca^{2+} sequestration mechanisms subsequently withdraw the released Ca^{2+} back into the SR and out of the cytosol (14, 15) reverting the cell to its relaxed state. Ca^{2+} also plays a central role in hypertrophic signalling. Hypertrophic stimuli such as endothelin-1 (ET-1) bind to G-protein-coupled receptors at the cell membrane to stimulate generation of the intracellular signalling molecule inositol 1,4,5-trisphosphate (IP_3). After IP_3 binds to and activates its cognate receptor, inositol 1,4,5-trisphosphate receptors (IP_3R), on the SR and nuclear envelope, Ca^{2+} is released into the cytosol and nucleus respectively (16, 17) (see Figure 1). This Ca^{2+} signal arising from IP_3R s has been shown in multiple mammalian species to produce a distinct Ca^{2+} signal that, through activation of pro-hypertrophic pathways including those involving NFAT, induces hypertrophy within cardiomyocytes. (16, 18, 19).

In healthy adult rat ventricular myocytes (ARVMs), various effects of IP_3 on global Ca^{2+} transients associated with ECC have been described, summarised in Table 1. While application of GPCR agonists that stimulate IP_3 generation produces robust effects on ECC associated IP_3 transients and contraction, the direct contribution of IP_3 to these actions varies between studies (17, 20–24). For example, in rabbit the effect of ET-1 on Ca^{2+} transient amplitude is sensitive to the IP_3R inhibitor 2-APB (22), whereas in healthy rats IP_3R inhibition with 2-APB was without effect (25). In mice 2-APB abrogated an increase in ECC associated Ca^{2+} transients brought about by AngII (24). Responses have also been variable when IP_3 was directly applied to cardiac myocytes. In healthy rat, IP_3 produced no or a modest effect on Ca^{2+} transient amplitude (17, 21), whereas in rabbit (22) a more substantial effect was observed. These differences in the effect of IP_3 have been ascribed in part to the greater dependence of rat myocytes on SR Ca^{2+} release to the Ca^{2+} transient than rabbit myocytes(22). Notably, both ET-1 and IP_3 elicit arrhythmogenic effects whereby they promote the generation of spontaneous calcium transients, manifest as a prolonged Ca^{2+} transient with additional peaks, and they increase the frequency of Ca^{2+} sparks (17, 18, 21, 22). A more profound role for IP_3 signalling is observed in hypertrophic ventricular myocytes, with ECC-associated Ca^{2+} transients of greater amplitude reported. Underlying these effects, IP_3R expression is elevated in hypertrophy (26). Hence, a question remains as to what independent effect IP_3R activation has on the cytosolic Ca^{2+} transient in healthy ventricular cardiac myocytes.

Cell State		IP_3	ET-1
Rat	Amplitude:	r▲ ⁽²¹⁾ r◆ ⁽¹⁷⁾	r▲ ⁽²¹⁾ r◆ ⁽¹⁶⁾ r▲ ⁽¹⁷⁾
	Duration:	–	–
	Basal Ca^{2+} :	r◆ ⁽¹⁷⁾	r◆ ⁽¹⁷⁾
	SCTs:	r▲ ⁽²¹⁾ r▲ ⁽¹⁷⁾	r▲ ⁽²¹⁾ r▲ ⁽¹⁷⁾
Other species	Amplitude:	m▲ ⁽²⁰⁾ m◆ ⁽²⁷⁾	h▲ ⁽²⁰⁾ m▲ ⁽²⁰⁾
	Duration:	–	–
	Basal Ca^{2+} :	m▲ ⁽²⁷⁾	m▲ ⁽²⁰⁾ b▲ ⁽²²⁾
	SCTs:	–	h▲ ⁽²⁰⁾ m▲ ⁽²⁰⁾

Table 1: Summary of experimentally observed changes to the Ca^{2+} transient in normal healthy ventricular myocytes in rat and other species following addition of IP_3 and ET-1. SCTs: spontaneous Ca^{2+} transients; ▲ indicates an increase; ▼ a decrease; ◆ indicates no significant change reported; r indicates rat, b indicates rabbit, h indicates human, m indicates mouse; dashes indicate no data found. The model developed in this work is primarily parameterised with rat data.

The individual behaviour of IP_3R channels and their dependence on Ca^{2+} , IP_3 , and ATP in cardiac and other cell types has

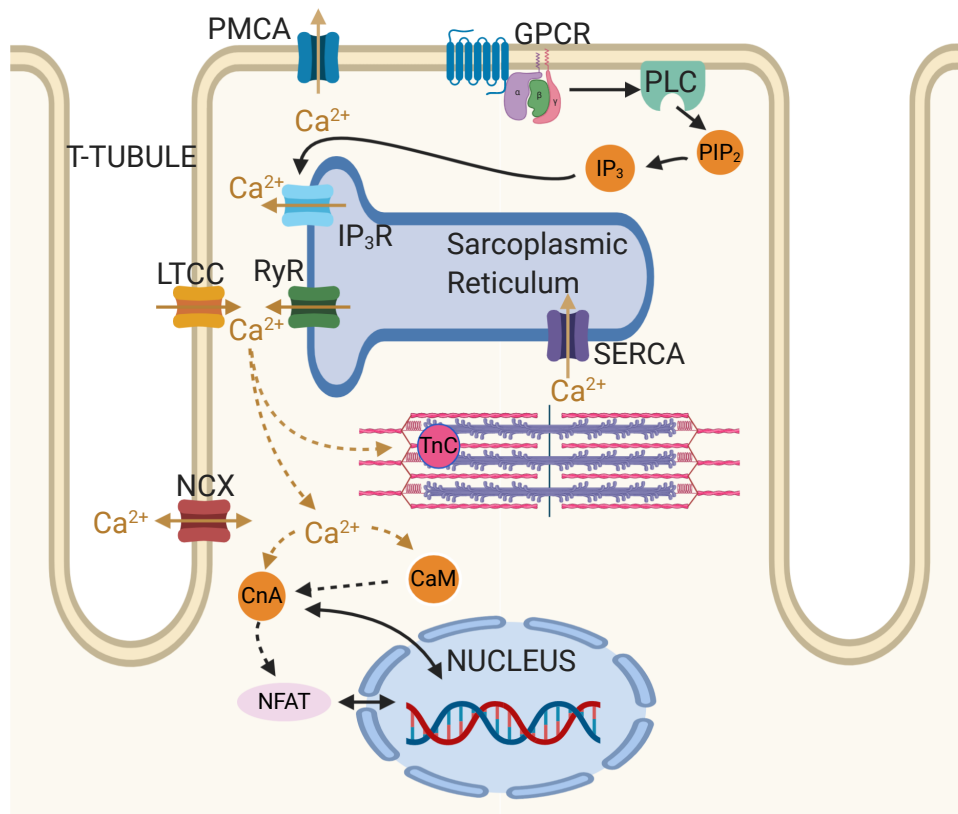


Figure 1: Schematic showing key Ca²⁺ signalling pathways in the cardiomyocyte. ECC processes include ryanodine receptors (RyR), L-type Ca²⁺ channel (LTCCs), sarco-endoplasmic reticulum Ca²⁺ ATP-ase (SERCA), sodium calcium exchanger (NCX), sarcolemmal calcium pump (PMCA) and Troponin-C (TnC). Growth-related IP₃- CnA/NFAT signalling processes include inositol 1,4,5-trisphosphate receptors (IP₃R), G protein-coupled receptor (GPCR), phospholipase C (PLC), phosphatidylinositol 4,5-bisphosphate (PIP₂), calmodulin (CaM), calcineurin (CnA) and nuclear factor of activated T-cells (NFAT).

been explored in a number of studies (28–31). These studies have formed the basis of several computational models of IP₃R type I isoforms (30, 32, 33) fitted to stochastic single-channel data (34). However, properties of IP₃R channel activity within the cardiomyocyte, such as gating state transition rates and their dependency on IP₃ and Ca²⁺, have not been directly measured. In this study we have taken the experimental studies on rat ventricular cardiomyocytes as a reference point for the observed effects of IP₃R activation on cellular Ca²⁺ dynamics and extended a well-established model of beat-to-beat cytosolic Ca²⁺ transients in rat cardiac cells (14, 35) to include a model of type II IP₃R (33) channels. This deterministic, compartmental model of ECC enables us to investigate biophysically plausible mechanisms by which IP₃R activation could affect Ca²⁺ dynamics at the whole cell scale, while avoiding the computational complexity associated with detailed stochastic and spatial modelling. Specifically, it enables us to explore the parameter ranges of IP₃R-mediated Ca²⁺ release that modify the global cytosolic Ca²⁺ transient to encode information for hypertrophic signalling to the nucleus.

A number of transcription factors transduce changes in Ca²⁺ to activate hypertrophic gene transcription. Of particular note is Nuclear Factor of Activated T-cells (NFAT). There are five known NFAT isoforms expressed in mammals, four of these are found in cardiac cells (19, 36). To initiate hypertrophic remodelling, the hypertrophic Ca²⁺ signal, in conjunction with calmodulin (CaM) and calcineurin (CnA) leads to dephosphorylation of cytosolic NFAT. Upon dephosphorylation NFAT translocates to the nucleus where, in coordination with other proteins, it activates expression of genes responsible for hypertrophy (37). Several studies have focused on characterising the Ca²⁺ dynamics necessary to activate NFAT and initiate hypertrophy (8, 19, 38–43) and have shown NFAT to be a Ca²⁺ signal integrator (38). Furthermore, a recent study by Hannanta-anan and Chow (8) used direct optogenetic control of cytosolic Ca²⁺ transients in HeLa cells to demonstrate that the transcriptional activity of NFAT4 (also known as NFATc3), a necessary NFAT isoform in the hypertrophic pathway (36), can be up-regulated by increasing the residence time of Ca²⁺ in the cytosol within each oscillation. The increased residence time of Ca²⁺, referred to as the ‘duty cycle’, is the ratio between the area under the Ca²⁺ transient curve divided by the maximum possible area, as calculated by the product of transient amplitude and period (see Figure 2A). The Ca²⁺ duty cycle is therefore distinct from the average Ca²⁺ concentration. Hannanta-anan and Chow (8) showed that increasing the duty cycle had a proportionally greater effect on NFAT transcriptional activity than changing either the frequency or amplitude of the cytosolic Ca²⁺ oscillations. This suggests an increased Ca²⁺ duty cycle as a possible mechanism by which Ca²⁺ release through IP₃R channels can effect hypertrophic signaling.

Here, using a mathematical model of beat-to-beat cytosolic Ca²⁺ transients in rat ventricular myocytes, coupled to IP₃R channel Ca²⁺ release, we show that IP₃R activation in the cytosol can increase the duty cycle of the cytosolic Ca²⁺ transient. We establish model feasibility through parameter sensitivity analysis, which shows that this behaviour does not depend sensitively on model parameter values. Furthermore we identify conditions necessary for IP₃R channel activation to alter Ca²⁺ transient amplitude, width, basal Ca²⁺ and duty cycle, as identified in different experimental studies, and compare model simulations to published experimental data summarised in Table 1. Finally, we couple simulations of cytosolic Ca²⁺ dynamics to a model of downstream CaM/CnA/NFAT activation and show that the duty cycle of the Ca²⁺ transient highly correlates with the activated nuclear NFAT (the proportion of NFAT which is dephosphorylated and translocated to the nucleus). These findings suggest IP₃R activity can increase the cytosolic Ca²⁺ duty cycle, thus providing a mechanism for IP₃-dependent activation of NFAT for hypertrophic signalling in the cardiomyocyte.

METHODS

We developed a computational model of RyR- and IP₃R-mediated Ca²⁺ fluxes in the adult rat ventricular myocyte. Model simulations were performed using the ode15s ODE solver from MATLAB 2017b (The MathWorks Inc., Natick, Massachusetts) with relative and absolute tolerances 1×10^{-3} and 1×10^{-6} respectively. The model equations were simulated at 1 Hz, the original pacing frequency of the Hinch et al. (14) model and at 0.3 Hz because it is another common pacing frequency in experimental studies of IP₃ and Ca²⁺ in cardiomyocytes (17, 21). The model was paced until the normalised root mean square deviation (NRMSD) between each subsequent beat was below 1×10^{-3} , and all but the last oscillation discarded to eliminate transient behaviours (see Figure 2B). Initial conditions were set to the basal Ca²⁺ level of the model at dynamic equilibrium with inactive IP₃R channels, determined after running the base model until the NRMSD was also below 1×10^{-3} .

Model Equations

The compartmental model of rat left ventricular cardiac myocyte Ca²⁺ dynamics is based on the Hinch et al. (14) model of ECC, with the addition of IP₃R Ca²⁺ release modelled using the Siekmann-Cao-Sneyd model (33). The Hinch model is an established whole cell model of rat cardiac Ca²⁺ dynamics that describes the flux through the major Ca²⁺ channels and pumps on the cell and SR membranes and the effects of applying a voltage across the cell membrane. The parameters for the Hinch component of our model were maintained from the original except for those of the driving voltage. This was shortened to better

approximate the rat action potential (44) (see Figure S1). The Ca²⁺ in the cytosol is governed by the following ODE:

$$\frac{d[\text{Ca}^{2+}]_{\text{cyt}}}{dt} = \beta_{\text{fluo}} \cdot \beta_{\text{CaM}} \cdot \left(I_{\text{CaL}} + I_{\text{RyR}} - I_{\text{SERCA}} + I_{\text{IP}_3\text{R}} + I_{\text{other}} \right) \quad (1)$$

$$I_{\text{other}} = I_{\text{SRl}} + I_{\text{NCX}} - I_{\text{PMCA}} + I_{\text{CaB}} + I_{\text{TnC}} \quad (2)$$

A small Ca²⁺ flux through the LTCCs, I_{CaL} , activates RyR channels to release Ca²⁺ from the SR into the cytosol at a rate of I_{RyR} . Ca²⁺ is resequenced into the SR by SERCA at a rate I_{SERCA} . β_{fluo} is the rapid buffer coefficient (45) for the fluorescent dye in the cytosol and β_{CaM} is the rapid buffer coefficient for calmodulin in the cytosol. I_{other} includes Ca²⁺ fluxes such as exchange with the extracellular environment through the sodium-calcium exchanger, I_{NCX} ; sarcolemmal Ca²⁺-ATPase, I_{PMCA} ; and the background leak current, I_{CaB} ; as well as the SR leak current, I_{SRl} ; and buffering on troponin C, I_{TnC} . These fluxes are defined in the SI (section 1).

When the simulation is run with IP₃ present, there is additionally a flux through the IP₃Rs :

$$I_{\text{IP}_3\text{R}} = k_f \cdot N_{\text{IP}_3\text{R}} \cdot P_{\text{IP}_3\text{R}} \cdot \left([\text{Ca}^{2+}]_{\text{SR}} - [\text{Ca}^{2+}]_{\text{cyt}} \right) / V_{\text{myo}} \quad (3)$$

Here V_{myo} is the volume of the cell. k_f is the maximum total flux through each IP₃R channel; this was chosen to be 0.45 $\mu\text{m}^3\text{ms}^{-1}$ unless otherwise stated to create a measurable effect on IP₃R channel activation while maintaining plausible total flux. $N_{\text{IP}_3\text{R}}$ is the number of IP₃R channels in the cell, this was set to 1/50th of the number of RyR channels (46). We studied the effect of varying k_f on IP₃-induced changes to the cytosolic Ca²⁺ transient in normal cardiomyocytes. Evidently, varying $N_{\text{IP}_3\text{R}}$ and varying k_f have the same effect on simulated calcium dynamics. While $N_{\text{IP}_3\text{R}}$ is known to increase significantly in disease conditions, we have not emphasised it in this study due to our focus on normal cardiomyocytes. $[\text{Ca}^{2+}]_{\text{cyt}}$ and $[\text{Ca}^{2+}]_{\text{SR}}$ are the Ca²⁺ concentrations in the cytosol and SR respectively.

$P_{\text{IP}_3\text{R}}$ is the [Ca²⁺] and [IP₃] dependent open probability of the IP₃R channels, and is determined using the Siekmann-Cao-Sneyd model (32, 33, 47), which has an in-built delay in response to changing Ca²⁺ concentration, along with several parameters governing channel activation and inactivation. This model describes $P_{\text{IP}_3\text{R}}$ as:

$$P_{\text{IP}_3\text{R}} = \beta / (\beta + k_\beta \cdot (\beta + \alpha)) \quad (4)$$

where k_β is a transition term derived from single-channel Siekmann et al. (47), β describes the rate of activation and α the rate of inactivation:

$$\beta = B \cdot m \cdot h \quad (5)$$

$$\alpha = (1 - B) \cdot (1 - m \cdot h_\infty) \quad (6)$$

where h is time-dependent, and B , m , and h/h_∞ describe the dependence on IP₃, the dependence on Ca²⁺ and the Ca²⁺-dependent delay in IP₃R gating, respectively. Expressions for these variables are as follows:

$$B = [\text{IP}_3]^2 / \left(K_p^2 + [\text{IP}_3]^2 \right) \quad (7)$$

$$m = [\text{Ca}^{2+}]^4 / \left(K_c^4 + [\text{Ca}^{2+}]^4 \right) \quad (8)$$

$$\frac{dh}{dt} = \left((h_\infty - h) \cdot \left(K_t^4 + [\text{Ca}^{2+}]^4 \right) \right) / \left(t_{\text{max}} \cdot K_t^4 \right) \quad (9)$$

$$h_\infty = K_h^4 / \left(K_h^4 + [\text{Ca}^{2+}]^4 \right) \quad (10)$$

Here K_c and K_h are parameters which determine the Ca²⁺-dependence of IP₃R channel open probability, while K_t and t_{max} are parameters which affect the delay in IP₃R response to cytosolic changes. K_t determines the influence of [Ca²⁺] on the delay, while t_{max} is a temporal scaling factor.

We note that the SR leak flux, I_{SRl} , is unchanged from the Hinch model, and would include the effects of diastolic IP₃R Ca²⁺ release at normal IP₃ levels as that model did not explicitly include IP₃R. However, in the presence of IP₃, IP₃R Ca²⁺ flux during diastole is several orders of magnitude greater than I_{SRl} , which is largely dependent on $[\text{Ca}^{2+}]_{\text{SR}}$, and hence any discrepancy caused by this will have a negligible effect on overall Ca²⁺ dynamics within the cell (see also Figure S4).

Several experimental studies have investigated IP₃R activity across a range of Ca²⁺ concentrations with 1 μM IP₃ (28, 48). These studies suggest that IP₃R channels would be open, with almost constant $P_{\text{IP}_3\text{R}}$ over the full range of cytosolic Ca²⁺

concentrations experienced during ECC in the cardiomyocyte. An IP₃R-facilitated SR-Ca²⁺ leak has been reported to amplify systolic concentrations (49, 50) as seen in most published experiments of IP₃ enhanced Ca²⁺ transients tabulated in Table 1. Through parameter sensitivity analysis of this model, we show that in order to be consistent with these observations P_{IP_3R} must be significantly smaller at resting Ca²⁺ concentrations than at higher concentrations.

Coupling cytosolic Ca²⁺ and NFAT activation

We coupled the calcium model to the NFAT model developed by Cooling et al. (51), which determines the proportion of total cellular NFAT that is dephosphorylated and translocated to the nucleus for a given cytosolic Ca²⁺ signal. In this study we have used the model parameters estimated from the data in Tomida et al. (38) who measured activation of NFAT4 in BHK cells. Full details of the Cooling et al. (51) model are given in the Supplementary Information.

RESULTS

An example of the model output when run with the original IP₃R channel parameter values determined by Sneyd et al. (33) for type I IP₃R channels is shown in Figure 2C. Measurements of the properties of IP₃R channel activity and their dependence on Ca²⁺ within cardiomyocytes are sparse in the literature. Therefore we performed a parameter sensitivity analysis by running model simulations over a variety of parameter ranges to explore the dependence of features of the cytosolic calcium transient to IP₃R channel parameters.

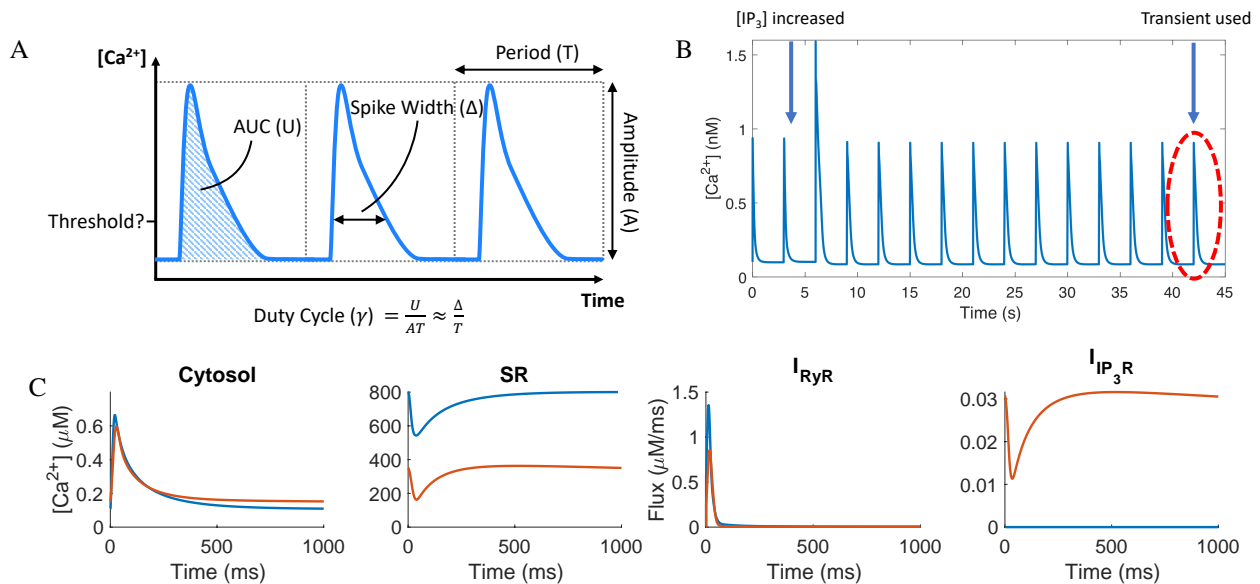


Figure 2: (A) The duty cycle, a function of AUC, amplitude, and period, for the cytosolic Ca²⁺ transient. (B) Example of Ca²⁺ transients generated by the model. (C) Ca²⁺ concentration in cytosol and SR, RyR flux, and IP₃R flux in the model with elevated IP₃ (red) and without IP₃ (blue). Here IP₃R parameters used are taken from Sneyd et al. (33), with maximum IP₃R flux $k_f = 0.003 \mu\text{M}^3 \text{ms}^{-1}$.

Parameter sensitivity analysis

We conducted a parameter sensitivity analysis to determine the critical parameters related to IP₃R activation that affect the shape of beat-to-beat cytosolic Ca²⁺ transients. We used the Jansen method (52) as described in Saltelli et al. (53) (and summarised in the SI) to calculate the ‘main effect’ and ‘total effect’ coefficients of each of the parameters associated with IP₃R channel gating in relation to changes in transient amplitude, full duration at half maximum (FDHM), diastolic Ca²⁺ and duty cycle (see Table 2). Saltelli et al. (53) describe the main effect coefficient as ‘the expected reduction in variance that would be obtained if [the parameter] could be fixed’ and the total effect coefficient as ‘the expected variance that would be left if all factors but [the parameter] could be fixed’, both normalised by the total variance. Both coefficients are included here to provide a complete picture of the impact of each parameter. Simulation parameter values were generated using the MATLAB sobolset function

with leap 1×10^3 and skip 1×10^2 .

Variance-based parameter sensitivity analysis

Main Effect Coefficients	[IP ₃]	t_{max}	K_c	K_h	K_f	k_f
Amplitude	0.27	0.00	0.03	0.19	0.00	0.03
FDHM	0.17	0.00	0.01	0.12	0.00	0.50
Diastolic Ca ²⁺	0.44	0.00	0.09	0.03	0.00	0.04
Duty Cycle	0.23	0.00	0.01	0.16	0.00	0.33
Total Effect Coefficients	[IP ₃]	t_{max}	K_c	K_h	K_f	k_f
Amplitude	0.63	0.04	0.43	0.46	0.02	0.13
FDHM	0.33	0.00	0.19	0.19	0.00	0.54
Diastolic Ca ²⁺	0.79	0.00	0.45	0.06	0.00	0.18
Duty Cycle	0.45	0.00	0.25	0.24	0.00	0.38

Table 2: Main and total effects of the IP₃R gating parameters on Ca²⁺ transient amplitude, duration (FDHM), diastolic Ca²⁺, and duty cycle. Significant values are highlighted in bold font.

Table 2 shows that the delay parameters t_{max} and K_f do not have a large effect on the cytosolic Ca²⁺ transient. While they are necessary to describe the effect of IP₃R-dominated Ca²⁺ dynamics (33), they contribute only a small amount to the variance. Therefore we decided to fix these parameters in our simulations.

As expected, the coefficients show that cardiac cell Ca²⁺ dynamics during ECC are most highly sensitive to IP₃ concentration ([IP₃]) and the maximal flux through each IP₃R (k_f). The maximal flux k_f has little effect on transient amplitude, but large influence on duration and duty cycle; while [IP₃] has the greatest effect on the change in amplitude and diastolic Ca²⁺ concentration.

The gating parameters K_c and K_h also influence the cytosolic Ca²⁺ transient. K_h affects the [Ca²⁺] at which IP₃R channels are inhibited and K_c affects the [Ca²⁺] at which IP₃R channels open. We illustrate how these two parameters affect IP₃R open probability, P_{IP_3R} , in Figure 3. Figure 3 also shows how [IP₃] affects the relationship between K_c , K_h , [Ca²⁺] and P_{IP_3R} . It can be seen that with $K_h = 80$ nM, P_{IP_3R} will be close to zero regardless of the values of Ca²⁺ or [IP₃] or K_c . At $K_h = 1.6$ μ M and [IP₃] ≥ 5 μ M P_{IP_3R} dependence on K_c and Ca²⁺ becomes apparent. Finally, at $K_h = 3.2$ μ M, P_{IP_3R} is still dependent on K_c and Ca²⁺ values, but [IP₃] does not change P_{IP_3R} significantly.

From this analysis, we determine that in order for IP₃R channels to be active during ECC, K_h must be sufficiently high that IP₃Rs are not inhibited at diastolic [Ca²⁺]. Conversely, K_c must be low enough that IP₃R channels are active at Ca²⁺ concentrations below the systolic Ca²⁺ peak. Therefore, in the remainder of this study, we fix K_h at 2.2 μ M: high enough to fulfill this condition while low enough that IP₃R channels are still affected by [IP₃]. We report simulation results only within the range of K_c that exhibits experimentally plausible Ca²⁺ transient properties.

With the plausible range of K_h and K_c established, we next show the effect of K_c , k_f and [IP₃] on the ECC transient.

IP₃ concentration and IP₃R opening behaviour have the greatest impact on the Ca²⁺ transient

As summarised in Table 1, different experimental studies suggest different effects of IP₃R activation on the ECC cytosolic Ca²⁺ transient. Figures 4A-C show quantitative predictions of how much Ca²⁺ transient properties could be affected by IP₃R activation across a range of [IP₃] and Ca²⁺-dependent IP₃R gating parameter K_c values. k_f was fixed at 0.45 μ m³ms⁻¹ and K_h was fixed at 2.2 μ M.

The red region in Figure 4A corresponds to IP₃R activation parameters that produce the greatest increase in Ca²⁺ amplitude. Noteworthy is that the red region depicts moderate changes in amplitude of $\sim 15\%$. This region corresponds to K_c values greater than 4 μ M and [IP₃] greater than 2 μ M. With K_h set at 2.2 μ M, this corresponds to the middle and far-right plots of P_{IP_3R} in Figure 3. The middle subfigure shows that with K_c greater than 4 μ M IP₃R channels would open only at Ca²⁺ concentrations greater than the diastolic concentration of ~ 0.1 μ M. The plot also shows that IP₃Rs would remain active at Ca²⁺ greater than the systolic peak concentration of ~ 1 μ M (54). Figure 4B further indicates that the increase in peak amplitude is accompanied by an increase in transient duration (FDHM). However, this change may be small, particularly at IP₃ concentrations lower than 1 μ M. In Figure 4C it can be seen that the diastolic Ca²⁺ concentration decreases moderately ($\sim 10\%$) in the parameter range where the amplitude is maximised (Figure 4A).

Figure 4B shows that FDHM of the Ca²⁺ transient increases whenever IP₃Rs are active. This increase is greater with greater

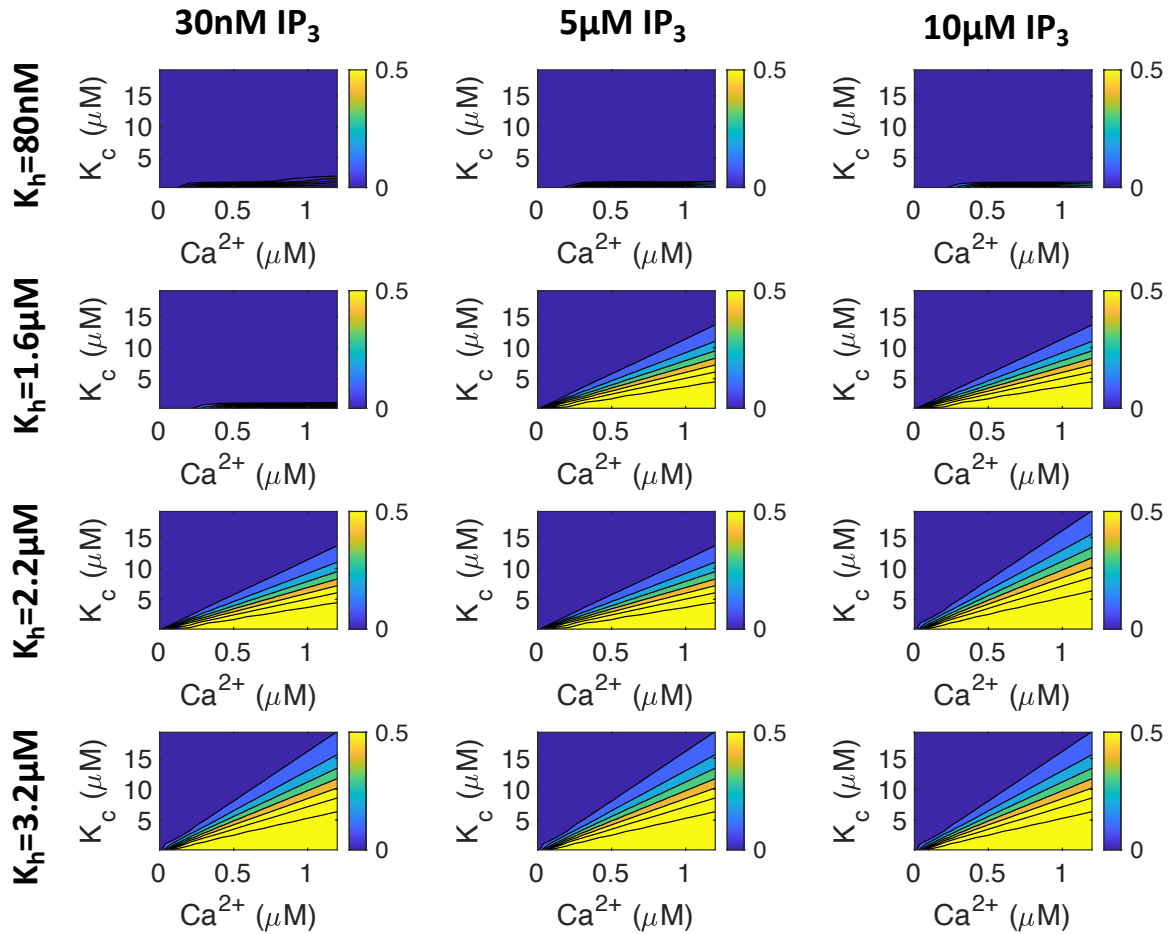


Figure 3: The effect of [Ca²⁺], [IP₃], K_c, and K_h on P_{IP_3R} in the Siekmann-Cao-Sneyd IP₃R model (32, 33, 47). The coloured bars on the side of each plot show the proportion of IP₃R channels that will open for each set of parameters at steady state. Note that IP₃Rs do not open at physiological Ca²⁺ concentrations when K_h is low (i.e. 80 nM or less). In subsequent simulations we used the value K_h = 2.2 μM unless otherwise stated.

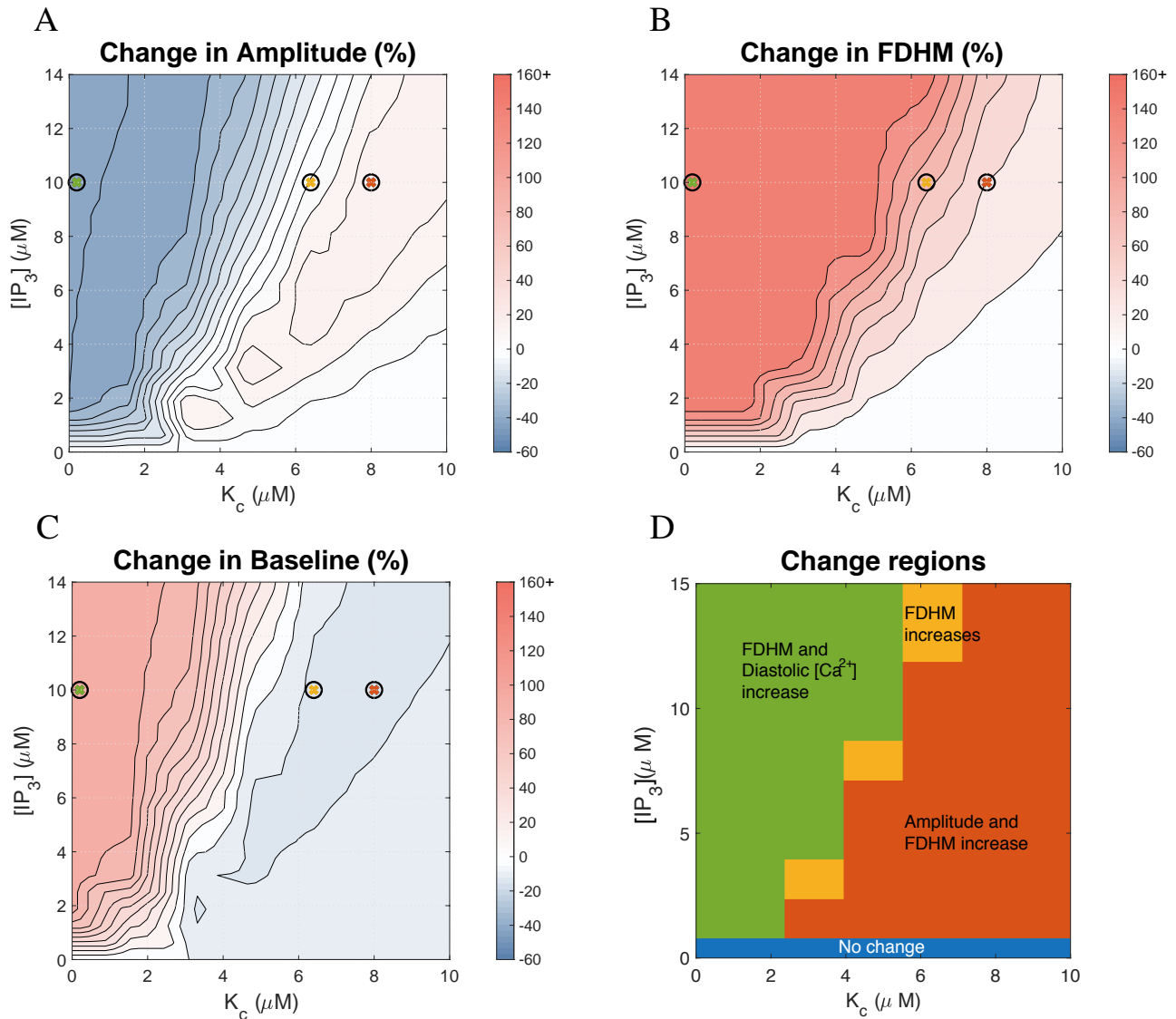


Figure 4: Effect of IP₃ concentration and the parameter K_c on the Ca²⁺ transient with pacing frequency 1 Hz. These two parameters, along with maximum IP₃R flux, k_f have the greatest impact when considering the effect of IP₃R activation on the Ca²⁺ transient. To better resolve the range in which FDHM changes, all FDHM increases of 45% and over are shown in the same colour. See Figure 5 for simulated transients at parameters indicated by crosses. We note that for ease of comparison between figures, in this and in subsequent figures the maximum increase from baseline is cropped at 160%. Changes greater than this threshold are shown in the same colour.

concentrations of IP_3 and with lower values of K_c . Figure 4C indicates that K_c and $[IP_3]$ have a similar effect on the diastolic Ca^{2+} concentration except that the location of the red and orange cross predicts a small ($\sim 10\%$) drop in diastolic Ca^{2+} . In all three Figures (A-C) there is little change when $[IP_3]$ is low and K_c is high (bottom right corner of each image). This is a regime in which the IP_3R channels barely open in response to ECC transients. For comparison, Supplementary Figure S2 shows the same simulations as Figure 4 at a commonly used experimental pacing frequency of 0.3 Hz, showing similar trends.

In order to compare our simulation results with the experimental observations summarised in Table 1 we divided the parameter space shown in Figures 4A-C into four regions, shown in Figure 4D. In the red region, amplitude and FDHM increase. In the orange region only FDHM increases. In the green region FDHM and diastolic $[Ca^{2+}]$ increase but amplitude decreases. Comparing to the experimental observation of amplitude increase summarised in Table 1, the red region appears to describe the most plausible parameter range. Figure 4D also shows that there is no parameter set where both amplitude and diastolic Ca^{2+} concentration increase. Furthermore, there is no region in which transients with increased amplitude and decreased duration are observed, as has been reported in ET-1 treated rat ventricular myocyte experiments (55). Finally, with the exception of the blue region in which there is no change, we observe that the FDHM increases in all parameter regimes.

To examine these results further, we investigated model behaviour in different regions of Figure 4D, shown in Figure 5 and marked as green, red and orange crosses in Figure 4A-C. Comparing the green cytosolic profiles (corresponding to the green region in Figure 4D) and blue cytosolic Ca^{2+} profiles (corresponding to no IP_3R activation) in Figure 5, we find that IP_3R opening at diastolic Ca^{2+} levels and IP_3R inhibition at Ca^{2+} levels below peak transient concentrations generates a flatter Ca^{2+} transient. This is the result of a gradual depletion of SR Ca^{2+} stores from IP_3R s opening. This subsequently leads to lower Ca^{2+} release through RyR and IP_3R channels.

Interestingly, a delayed time to peak is observed with IP_3R activation in all regimes selected. With the reduction in SR load due to IP_3R activation, we find reduced Ca^{2+} flux through RyRs. In order to maintain or increase Ca^{2+} transient amplitude after activation, the IP_3R channels must compensate for the drop in RyR flux. As the spike in IP_3R flux is in response to Ca^{2+} release from RyR channels, and initial RyR-mediated Ca^{2+} release is slower with lower SR Ca^{2+} stores, it delays the time between cell stimulation and Ca^{2+} transient peak.

The increase in FDHM of the transient from IP_3R activation apparent in Figure 4B can be explained by continued release of Ca^{2+} through IP_3R channels after RyRs have closed in Figure 5. The slower release through IP_3R channels after RyRs close is a result of a smaller proportion of the channels opening and a decrease in SR Ca^{2+} store load.

Maximum flux through IP_3R s can increase signal duration

The parameter sensitivity analysis in Table 2 indicates that maximum flux through IP_3R s (k_f) has the greatest effect on Ca^{2+} transient duration. Therefore we next examined how increased k_f values in our model affects the Ca^{2+} transient. Figure 6A-C show that for $K_c < 2 \mu M$, increasing k_f above $0.45 \mu m^3 ms^{-1}$ mostly increases transient duration but has only marginal effects on amplitude and baseline. However for large K_c , the role of k_f in modifying transient shape becomes more noticeable. There is a clear region where amplitude increases (red region), however this is more dependent on K_c than k_f . At 1 Hz, there is no value of k_f that reduces transient duration. With IP_3R activation the transient duration increases and k_f merely determines by how much. However it is of note that, as shown in Figure 7, at a lower frequency of 0.3 Hz, when $k_f > 1.2 \mu m^3 ms^{-1}$ and $K_c > 8 \mu M$, there is a decrease in duration of the transient.

To compare simulation results to experimental observations in Table 1, we divided the parameter space shown in Figures 6A-C into three regions, shown in Figure 6D. The regions in this figure are consistent with the regions labelled in Figure 4D. Figure 7D shows similar regions corresponding to simulations at 0.3 Hz. It can be seen that at 0.3 Hz, $K_c > 8 \mu M$ and $k_f > 1.2 \mu m^3 ms^{-1}$ provide transients with increased amplitude and decreased duration, consistent with rat ET-1 experiments summarized in Table 1. However this value of k_f results in an unrealistic flux through IP_3R channels. Additionally, *in vivo*, the cell would be paced at a faster frequency and this result is unlikely without the cell being able to return to resting Ca^{2+} . We have not been able to identify a parameter set that would provide a simultaneous increase in both amplitude and diastolic Ca^{2+} .

RyR and IP_3R interaction increases the intracellular Ca^{2+} duty cycle

Having establishing reasonable parameters ranges for IP_3R activation based on the influence on ECC Ca^{2+} transient properties (amplitude, FDHM, and diastolic Ca^{2+}), we investigated the possibility that cytosolic Ca^{2+} plays a role in hypertrophic remodelling through changing the duty cycle. Given the time scale involved in hypertrophic remodelling, and the signal integration properties of NFAT, the IP_3R -modified cytosolic Ca^{2+} transient could cumulatively encode hypertrophic signalling. Using optogenetic encoding of cytosolic Ca^{2+} transients in HeLa cells, Hannanta-anan and Chow (8) demonstrated that the transcriptional activity of NFAT4 can be up-regulated by increasing cytosolic Ca^{2+} duty cycle. This is a plausible mechanism of signal encoding that is likely to be less susceptible to noise than either amplitude or frequency encoding. Therefore, we

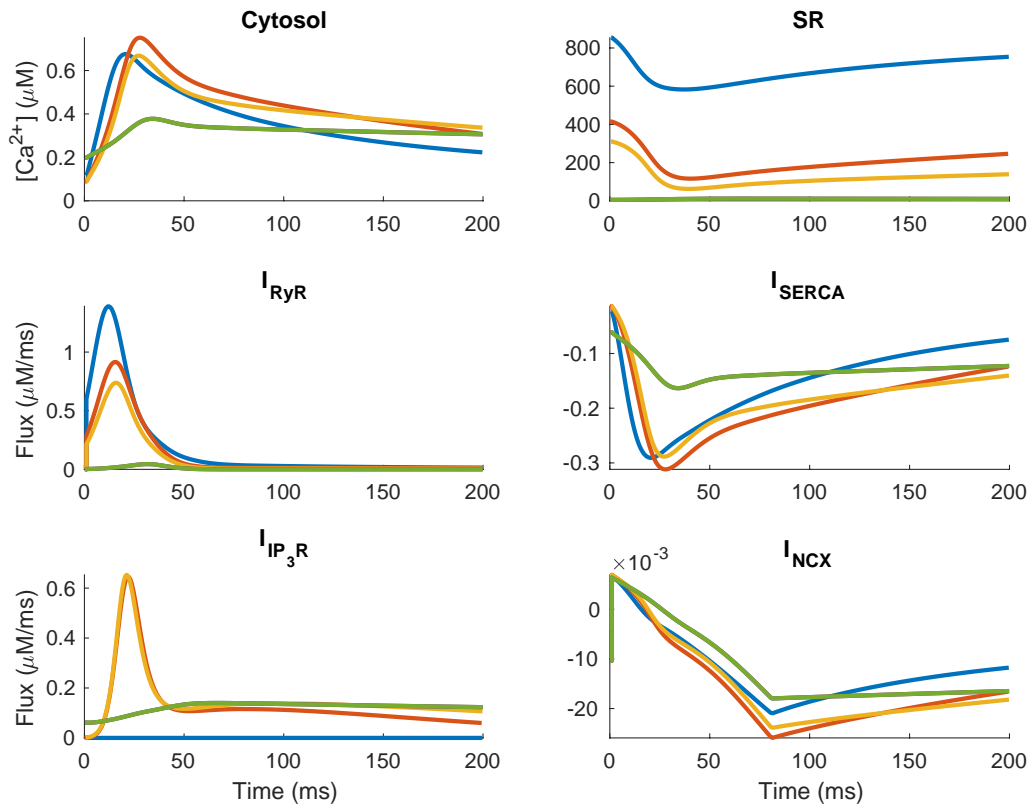


Figure 5: Simulated ECC transient and fluxes in the absence (blue) and presence of IP_3 , corresponding to low (green), medium (orange) and high (red) values of K_c . With $K_c = 8 \mu M$ (orange), IP_3R channels open only at Ca^{2+} concentrations greater than $0.1 \mu M$. This results in increased peak in cytosolic Ca^{2+} transients and depleted SR Ca^{2+} stores. Parameters here were selected to show: absence of IP_3R channels (blue), increased transient amplitude (orange, red) and IP_3R s parameterised as described in the original Siekmann-Cao-Sneyd model (green). IP_3 concentration is $10 \mu M$ and pacing frequency 1 Hz in all simulations. The sign of I_{NCX} indicates whether Ca^{2+} is moving into (positive) or out of (negative) the cell.

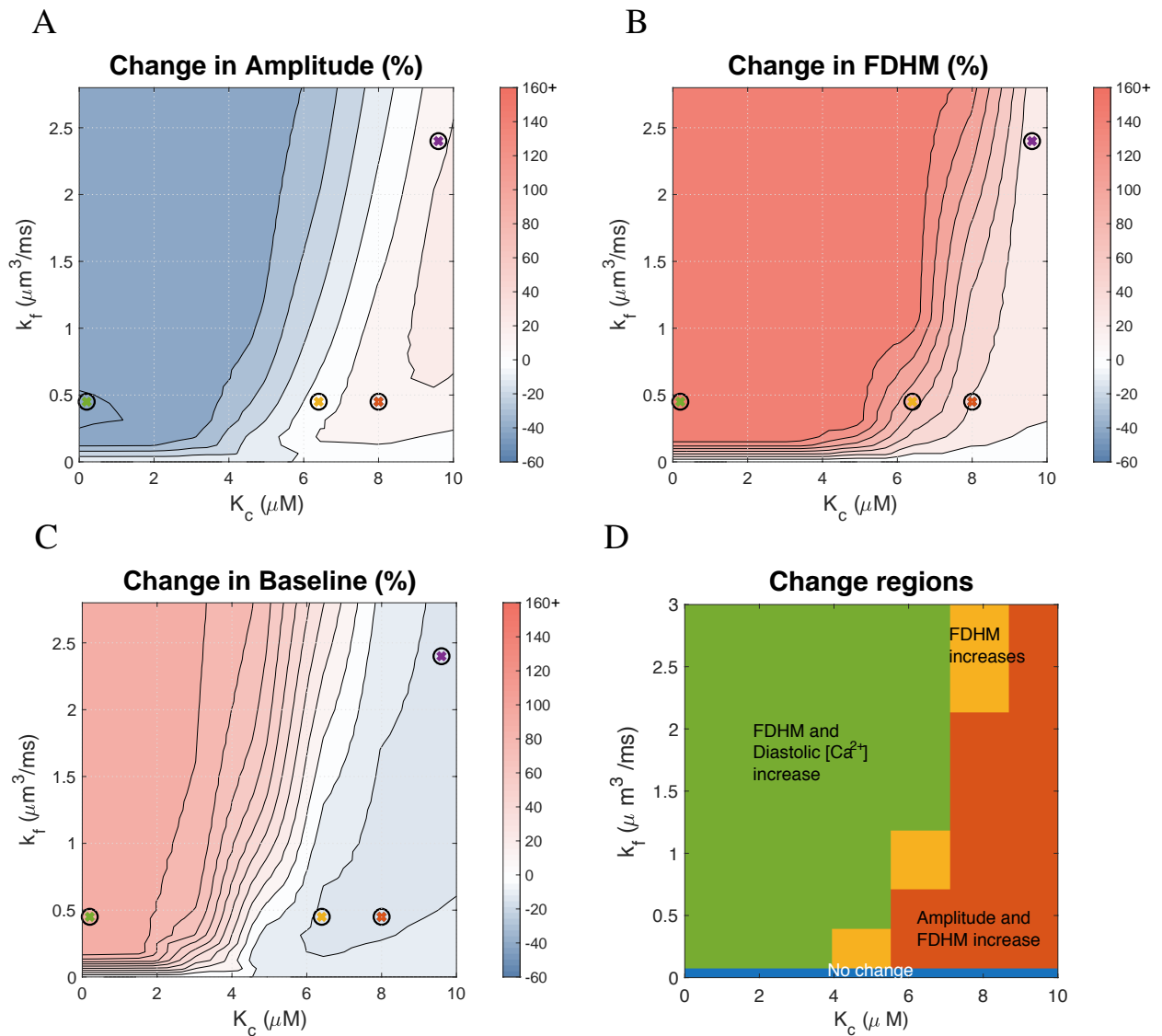


Figure 6: Effect of maximum IP₃R flux k_f and the Ca²⁺-sensitivity parameter K_c on the Ca²⁺ transient at 1 Hz. Maximum IP₃R flux has the greatest impact on transient duration. In these simulations $[\text{IP}_3] = 10 \mu\text{M}$. See Figure 5 for simulated transients at parameters indicated by crosses.

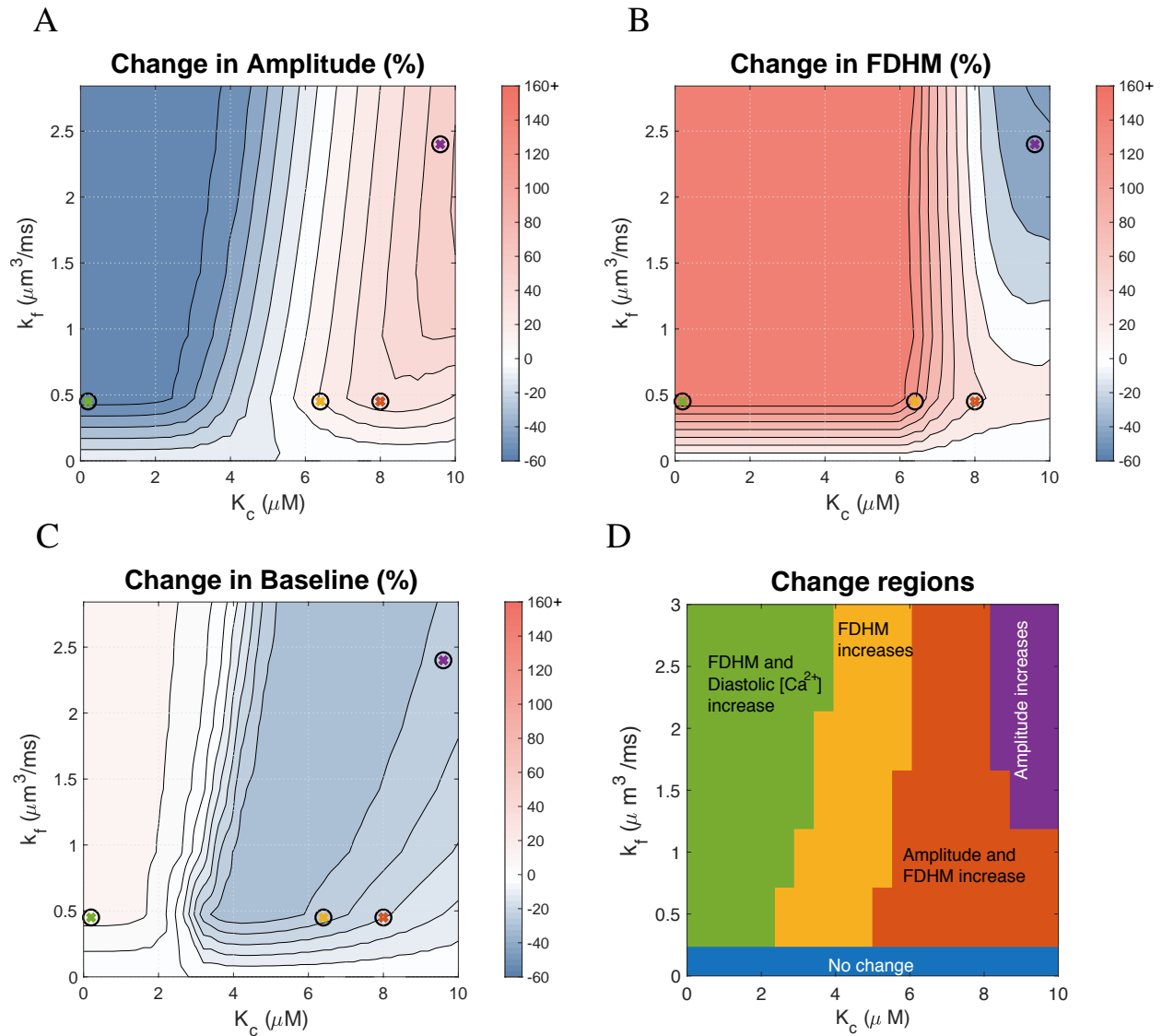


Figure 7: Effect of maximum IP₃R flux k_f and the Ca²⁺ sensitivity parameter K_c on the Ca²⁺ transient at 0.3 Hz. Maximum IP₃R flux has the greatest impact on transient duration. In these simulations $[\text{IP}_3] = 10 \mu\text{M}$. See Figure S3 for simulated transients at parameter values indicated by crosses.

examined the cytosolic Ca^{2+} duty cycle as a hypertrophic signalling mechanism.

We calculated the duty cycle for the Ca^{2+} transients in the plausible parameter ranges for IP_3R activation as the ratio between the area under the Ca^{2+} transient curve and the area of the bounded box defined by the amplitude and period of the Ca^{2+} transient (shown in Figure 2). Figure 8 shows the effects of $[\text{IP}_3]$, k_f , and K_c on the duty cycle of the cytosolic Ca^{2+} transient. The Figure shows that the Ca^{2+} duty cycle increases with IP_3R activation across the broad parameter range shown.

NFAT activation increases with an increase in calcium duty cycle

Having established that IP_3R activation results in increased calcium transient duty cycle, we coupled the model of cytosolic ARVM calcium dynamics to the model of NFAT activation developed by Cooling et al. (51). We then tested the effect of varying IP_3 concentration over a range of IP_3R parameter values on the proportion of dephosphorylated nuclear NFAT compared to that in the phosphorylated inactive state in the cytosol (Figure 9). These simulation data clearly show that increased IP_3 and alteration in Ca^{2+} transient duty cycle positively influences NFAT activation and thus provides a mechanism to couple IP_3 -induced Ca^{2+} release and activation of hypertrophic gene expression.

DISCUSSION

Here we have presented what is, to our knowledge, the first modelling study to investigate the effect of IP_3R channel activity on the cardiac ECC Ca^{2+} transient and possible information encoding mechanisms. We extended a well-established model of the ECC Ca^{2+} transient by Hinch et al. (14) to include a model of IP_3R activation and Ca^{2+} release. The model, upon IP_3R activation, simulates the influence of IP_3R activation on Ca^{2+} transients in non-hypertrophic adult rat left ventricular cardiac myocytes.

Parameter sensitivity analysis (Table 2) showed the maximal IP_3 -induced Ca^{2+} release through individual IP_3R (k_f) had the greatest influence on the Ca^{2+} transient duration and duty cycle. $[\text{IP}_3]$ had the biggest influence on the Ca^{2+} amplitude and diastolic Ca^{2+} concentration. We found that under fixed maximum IP_3R flux, $k_f = 0.45 \mu\text{m}^3\text{ms}^{-1}$, IP_3R activation increases the duration of the Ca^{2+} transient, but Ca^{2+} amplitude is IP_3 -dependent. The Ca^{2+} transient duration can be reduced only by increasing k_f to physiologically unrealistic values.

The finding that the Ca^{2+} transient duty cycle increases with $[\text{IP}_3]$ (see Figure 8) provides a plausible explanation for the mechanism by which IP_3 -dependent Ca^{2+} release from IP_3Rs can enhance pro-hypertrophic NFAT activity.

Does IP_3 -induced Ca^{2+} release modify the ECC transient?

Figures 4, 6 and 7 show that IP_3Rs can influence the ECC Ca^{2+} transient and the effect is dependent on the IP_3R properties and IP_3 concentration. Our model simulations predict that Ca^{2+} transient amplitude increases approximately 15% when IP_3R properties are such that IP_3Rs remain inhibited from opening at diastolic Ca^{2+} but release Ca^{2+} once RyRs are activated and remain open when Ca^{2+} concentration is above $1 \mu\text{M}$. The IP_3R parameter combination marked by a red cross in the contour plots is a representative example of this type of effect of IP_3Rs . There is also a narrow parameter range at $[\text{IP}_3]$ of $10 \mu\text{M}$ ($K_h = 2.2 \mu\text{M}$, $K_c = 6 \mu\text{M}$) where the amplitude does not change more than 5% (see Figure 4). The orange cross marks an example of IP_3R effects in this parameter range. These simulation predictions are consistent with the experimental studies that either show increased amplitude or no change in amplitude (Table 1).

Model simulations predict that IP_3R activation only increases diastolic $[\text{Ca}^{2+}]$ when IP_3R are open at resting $[\text{Ca}^{2+}]$ of $\sim 0.1 \mu\text{M}$ (see Figure 4D). Harzheim et al. (17) reported no measurable differences in diastolic $[\text{Ca}^{2+}]$ between ARVMs stimulated with an agonist, known to induce hypertrophy in healthy ARVMs, and those treated with a saline buffer (although effects have been observed in disease ventricular cardiomyocytes and atrial cardiomyocytes). Examination of simulated Ca^{2+} transients within a regime that results in diastolic $[\text{Ca}^{2+}]$ increase (green traces in Figure 5) shows that the transients do not resemble any of the observed experimental measurements in the literature. Therefore the comparison of model simulations and experimental measurements of diastolic $[\text{Ca}^{2+}]$ and Ca^{2+} transient amplitude suggest that the most likely regime of IP_3R activation lies between the orange and red regions in Figure 4D. Using these comparisons we propose that IP_3R activation makes modest changes to the ECC Ca^{2+} transient which are often hidden within the measurement variability in experiments.

The biological significance of the duty cycle

We showed that while amplitude, duration, and diastolic Ca^{2+} can increase or decrease depending on IP_3R parameter values and pacing frequency, the duty cycle, as defined by Hannanta-anan and Chow (8) always increases with IP_3 , consistent with effects seen in (21). The implication of this observation is that IP_3R activation is sufficient to provide a signal to drive NFAT nuclear translocation and hence hypertrophic gene expression in the manner described by Hannanta-anan and Chow (8).

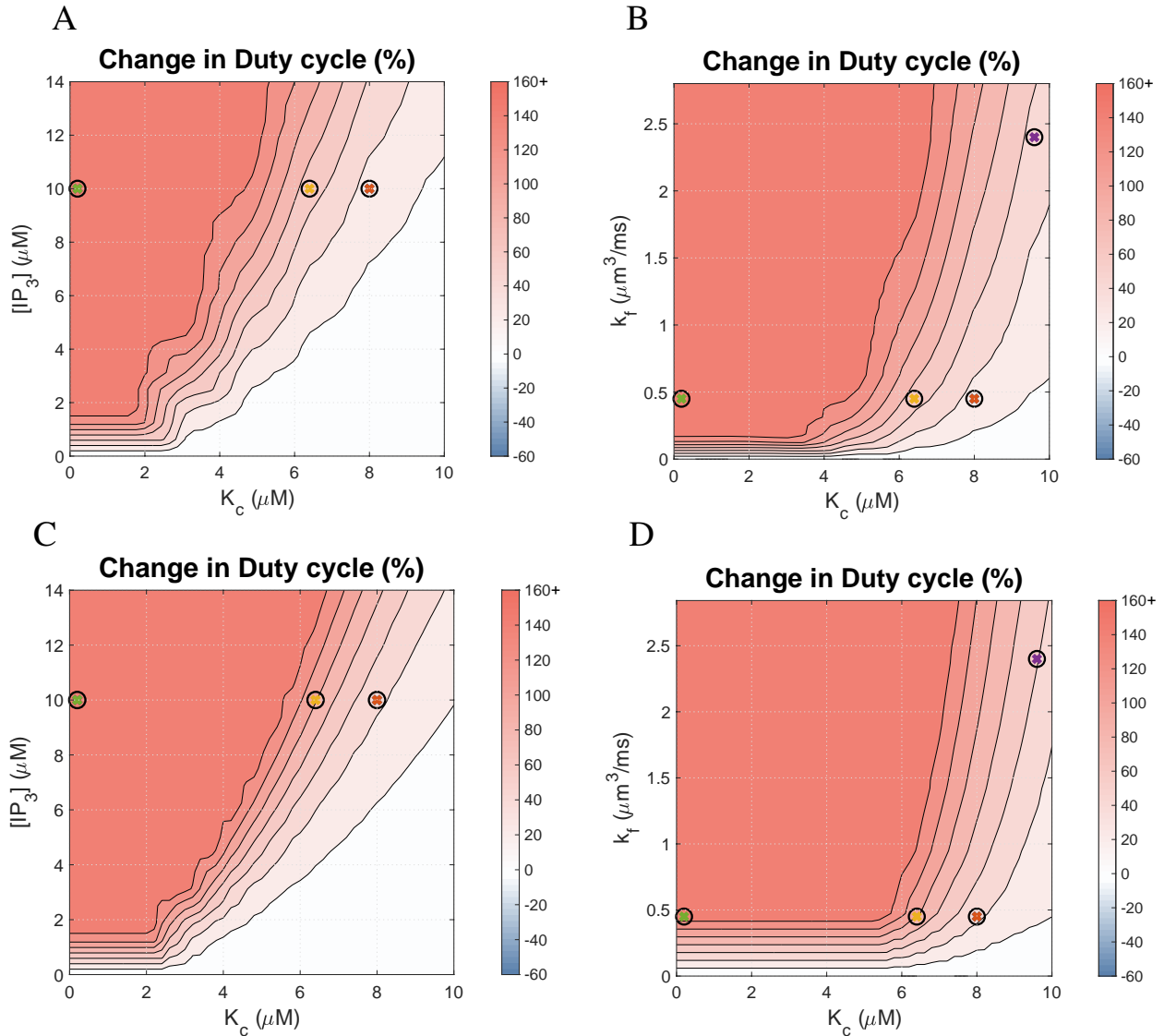


Figure 8: Effects on the Ca²⁺ transient duty cycle of (A) IP₃ concentration and the Ca²⁺ sensitivity parameter K_c with pacing frequency 1 Hz; (B) of maximum IP₃R flux k_f and K_c with pacing frequency 1 Hz; (C) of IP₃ concentration and K_c with pacing frequency 0.3 Hz; and (D) of maximum IP₃R flux k_f and the K_c at pacing frequency 0.3 Hz. The colour bar indicates the % change from a simulation run with identical parameters but no IP₃R channels. The coloured crosses indicate the parameters used for the corresponding plots in Figure 5. Hannanta-anan and Chow (8) report a transcription rate increase of approximately 30% with a duty cycle increase of 50% in Figure 2 of their paper. The duty cycle of the Ca²⁺ transient when IP₃Rs are inactive is 0.127.

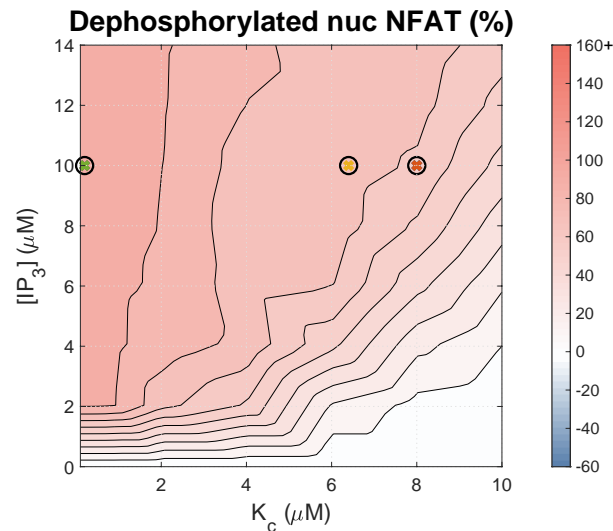


Figure 9: Effect of $[IP_3]$ and K_c on the concentration of dephosphorylated nuclear NFAT ($NFAT_n$). Simulations were paced at 1 Hz. The colour bar indicates the % change from a simulation run with identical parameters but no IP_3 .

Hannanta-anan and Chow (8) found that, when comparing Ca^{2+} oscillations of the same amplitude, oscillations with greater duty cycle had a greater effect on NFAT dephosphorylation and translocation to the nucleus. In their study, duty cycle, γ , was calculated as the area under the curve, U , divided by the maximum area under the curve (for Ca^{2+} oscillations of the same amplitude, A , and period of oscillation, T), i.e. $\gamma = U/AT$ (see Figure 2A). An alternative definition is $\gamma = \Delta/T$, where Δ is the transient duration and T the period of oscillation. This alternate formulation is used by Tomida et al. (38) and Salazar et al. (56) but is less well defined for analogue signals. The duty cycle in Figure 8 was calculated using the former definition. This can be compared with the latter definition when remembering that duty cycle will now vary with FDHM (Figures 4C and 6C).

The duty cycle in this system essentially reflects the fraction of each period of the Ca^{2+} cycle for which cytosolic Ca^{2+} is sufficiently elevated to affect the downstream proteins in the CnA/NFAT signalling pathway. The greater sensitivity of NFAT to Ca^{2+} oscillations with sustained elevation in intracellular Ca^{2+} is well established (19, 39, 57). While it is difficult to determine where this threshold is, NFAT is a Ca^{2+} integrator and a clear correlation has been found between Ca^{2+} duty cycle and NFAT activation (8). Increasing duty cycle increases the time NFAT spends in the dephosphorylated state, which is required to both enter and maintain it in the nucleus and hence effect transcription (58); NFAT responds to changes in duty cycle while being insensitive to both amplitude and frequency changes. We see in simulations too that the proportion of NFAT that is in the dephosphorylated nuclear state is highest when the duty cycle of the Ca^{2+} transient is high (Figures 8 and 9).

In experiments, IP_3 stimulation has been shown to lead to an increase in systolic Ca^{2+} in cardiac cells, but significant change in duration has not been reported (although as in Harzheim et al. (17) and Proven et al. (21), increased spontaneous calcium transients are observed which could function to prolong the duration of the Ca^{2+} transient). Based on the definition of the duty cycle presented in Hannanta-anan and Chow (8), there is a negative effect on duty cycle, and hence NFAT activation, when Ca^{2+} transient amplitude is increased. However, within the physiologically plausible parameter range we find that simulations with increased Ca^{2+} transient amplitude also have increased transient duration. We postulate that NFAT may be responsive to the Ca^{2+} transient through the latter definition of the duty cycle – i.e. the duration of time that Ca^{2+} is elevated over a threshold divided by the period. This is more consistent with both the biological mechanism and the potential increase in peak Ca^{2+} concentration in the hypertrophic pathway, which may be a side-effect of a corresponding increase in duration over this threshold. Further research, both theoretical and experimental, is required in order to determine the validity of this assumption.

Figure 9 shows a strong correlation between $[Ca^{2+}]$ -dependent NFAT activation and Ca^{2+} transient duty cycle in the Cooling et al. (51) model: the correspondence between Figure 8A and Figure 9 is striking. A caveat, however, is that the original Cooling et al. (51) study showed that the NFAT model is also sensitive to any average increase in cytosolic calcium. Therefore, while increasing Ca^{2+} transient duty cycle is shown to be sufficient for NFAT activation in this model, further experimental validation is required to confirm this mechanism in cardiomyocytes.

Experimental evidence of an IP₃-induced increase in calcium duty cycle?

An increase in duty cycle without an increase in frequency requires an increase in transient duration. While this increase is observed in our simulations for a broad range of parameter values, it has not however been reported in experiments involving IP₃ stimulation. The possible reasons for this are many and varied, however, as discussed earlier, using different IP₃ concentrations to those that occur *in vivo* may result in different effects on the shape of the Ca²⁺ oscillations, leading to inconsistent observations. Furthermore, small variations in Ca²⁺ concentrations may not be experimentally discernible, or may be hidden by the effect of Ca²⁺-sensitive dyes (59). A small, but prolonged variation in transient duration can produce a comparatively large change in duty cycle. Hence it remains to be confirmed experimentally whether IP₃R-dependent Ca²⁺ flux does indeed lead to an increased Ca²⁺ duty cycle in cardiomyocytes.

Limitations of the study

In this study we have considered generation of voltage-driven cytosolic Ca²⁺ transients using deterministic models of each ion channel in a compartmental model. There are several physiological features of cardiomyocyte Ca²⁺ dynamics which are not represented, and hence not considered in this approach. In particular, our model does not represent any of the stochastic events associated with IP₃R channels. Further modelling of combined stochastic channel gating may be necessary to elucidate the entire impact of IP₃R interaction with the cytosolic Ca²⁺ machinery. While cell structure is known to play a role in cardiac Ca²⁺ dynamics (60–62), effects beyond the synchronising function of the dyad are not considered in this compartmental study. Furthermore we have not considered the spatial IP₃R distribution. Our model is developed primarily using parameters fitted by Hinch et al. (14) and Sneyd et al. (33), and makes no distinction between IP₃R channels located within or outside the dyad (63, 64). These and other structural features of the cell could alter the Ca²⁺ available to regulate IP₃R channels and may be detected in the Ca²⁺ transient. Distinct effects of IP₃ signalling in the cytosol and the nucleus are also not considered. Cytosolic Ca²⁺ is thought to promote translocation of NFAT into the nucleus, while nuclear Ca²⁺ maintains it there (16). We have only investigated the former role for Ca²⁺ signalling within the CnA/NFAT pathway.

We have explored model behaviour at pacing frequencies of 1 Hz and 0.3 Hz, rather than higher, more physiological frequencies, primarily because the majority of parameters were derived from *in vitro* experiments conducted at room temperature. Extrapolation of parameters and hence model behaviour to *in vivo* temperature and correspondingly higher pacing frequency remains challenging. Therefore model predictions must be interpreted cautiously in relation to higher pacing frequencies.

Additionally, not all components of this signalling pathway have been considered in this study. Ca²⁺/calmodulin-dependent kinases II and Class IIa histone deacetylases, for example, are both known Ca²⁺-mediated components of the hypertrophic pathway that are activated by IP₃ signalling (65) but are not included. Here we have focused only on the impact of IP₃R activation on the cytosolic Ca²⁺ dynamics and how this relates to the mechanism of NFAT activation. In order to explore broader context for IP₃ mediated hypertrophic signalling, it remains to couple this model to upstream events including models of IP₃ production through activation of cell membrane receptors (66, 67). This would allow the profile and extent of the rise in IP₃ concentration due to the activation of the hypertrophic pathway in cardiomyocytes to be determined. We have focused on the effect of an elevated IP₃ concentration of 10 μM as many experimental studies into the effect of IP₃ on Ca²⁺ dynamics use saturating [IP₃]. However, Remus et al. (68) found stimulation of adult cat ventricular myocytes with 100 nM ET-1 induced a cell-averaged increase in IP₃ concentration of only 10 nM indicating a much lower concentration than used in experiments. This, together with known differences between species, suggests the IP₃ concentration detected by IP₃R receptors in ARVMs *in vivo* could be lower than the simulated 10 μM. However we note qualitatively similar effects on the Ca²⁺ transient in parameter regimes with lower [IP₃] in our model (Figures 4 and S2) albeit with more modest effects on the transient shape. Additionally, ET-1 receptors are localised to t-tubule membranes (69) so IP₃ may be generated very close to IP₃R channels (64, 70), increasing the concentration they detect.

Finally, IP₃R-induced Ca²⁺ release is a part of a larger hypertrophic signalling network. It remains to couple this model to other signalling pathways involved in bringing about hypertrophic remodelling (71). How cytosolic Ca²⁺ interacts with nuclear Ca²⁺ in regulation of NFAT nuclear residence and activity also remains to be determined.

Conclusion

The sensitivity of NFAT translocation to the Ca²⁺ duty cycle demonstrated by Hannanta-anan and Chow (8) raises the question as to whether IP₃R flux can increase the Ca²⁺ duty cycle in cardiomyocytes during hypertrophic signalling. Here we have shown using mathematical modelling that an increase in cytosolic Ca²⁺ transient duration can occur following addition of IP₃, and furthermore that this increase is sufficient to increase NFAT activation. Together, these results suggest a plausible mechanism for hypertrophic signalling via IP₃R activation in cardiomyocytes. While it cannot be ruled out that a significant role is played by components of this pathway that are not considered here, the computational evidence provided in this study,

along with the previous experimental findings, suggests encoding of the hypertrophic signal through alteration of the duration of cytosolic Ca^{2+} oscillations to be a feasible mechanism for IP_3 -dependent hypertrophic signalling.

AUTHOR CONTRIBUTIONS

EJC, VR, HLR, CS, and GB conceived of the study; EJC and VR supervised the project; HH, AT, VR and EJC developed the modelling approach. HH implemented the simulations. HLR, CS, and GB provided critical feedback. All authors contributed to writing the manuscript.

ACKNOWLEDGEMENTS

This research was supported in part by the Australian Government through the Australian Research Council Discovery Projects funding scheme (project DP170101358). HLR wishes to acknowledge financial support from the Research Foundation Flanders (FWO) through Project Grant G08861N and Odysseus programme Grant 90663.

SUPPORTING CITATIONS

References (72, 73) appear in the Supporting Material.

REFERENCES

1. Berridge, M. J., M. D. Bootman, and H. L. Roderick, 2003. Calcium signalling: dynamics, homeostasis and remodelling. *Nat. Rev. Mol. Cell Biol.* 4:517–529.
2. Clapham, D., 2007. Calcium Signaling. *Cell* 131:1047–1058.
3. Berridge, M., 1997. The AM and FM of calcium signalling. *Nat.* 386:759–760.
4. Berridge, M., 2006. Calcium microdomains: organization and function. *Cell Calcium* 40:405–412.
5. Bootman, M., C. Fearnley, I. Smyrniak, F. MacDonald, and H. L. Roderick, 2009. An update on nuclear calcium signalling. *J. Cell Sci.* 122:2337–2350.
6. Purvis, J. E., and G. Lahav, 2013. Encoding and Decoding Cellular Information through Signaling Dynamics. *Cell* 152:945–956.
7. Uzhachenko, R., A. Shanker, and G. Dupont, 2016. Computational Properties of Mitochondria in T Cell Activation and Fate. *Open Biol.* 6:160192.
8. Hannanta-anan, P., and B. Y. Chow, 2016. Optogenetic Control of Calcium Oscillation Waveform Defines NFAT as an Integrator of Calcium Load. *Cell Syst.* 2:283–288.
9. Roderick, H. L., D. Higazi, I. Smyrniak, C. J. Fearnley, D. Harzheim, and M. D. Bootman, 2007. Calcium in the heart: when it's good, it's very very good, but when it's bad, it's horrid. *Biochem. Soc. Trans.* 35:957.
10. Hohendanner, F., J. T. Maxwell, and L. A. Blatter, 2015. Cytosolic and Nuclear Calcium Signaling in Atrial Myocytes: IP_3 -Mediated Calcium Release and the Role of Mitochondria. *Channels* 9:129–138.
11. Zinn, M., S. West, and B. Kuhn, 2018. Mechanisms of Cardiac Hypertrophy. In J. L. Jefferies, A. C. Chang, J. W. Rossano, R. E. Shaddy, and J. A. Towbin, editors, *Heart Failure in the Child and Young Adult*, Academic Press, Boston, 51 – 58.
12. Tham, Y. K., B. C. Bernardo, J. Y. Y. Ooi, K. L. Weeks, and J. R. McMullen, 2015. Pathophysiology of cardiac hypertrophy and heart failure: signaling pathways and novel therapeutic targets. *Arch. of Toxicol.* 89:1401–1438.
13. Gilbert, G., K. Demydenko, E. Dries, R. D. Puertas, X. Jin, K. Sipido, and H. L. Roderick, 2019. Calcium Signaling in Cardiomyocyte Function. *Cold Spring Harb. Perspect. in Biol.* a035428.
14. Hinch, R., J. L. Greenstein, A. J. Tanskanen, L. Xu, and R. L. Winslow, 2004. A Simplified Local Control Model of Calcium-Induced Calcium Release in Cardiac Ventricular Myocytes. *Biophys. J.* 87:3723–3736.

15. Vierheller, J., W. Neubert, M. Falcke, S. H. Gilbert, and N. Chamakuri, 2015. A multiscale computational model of spatially resolved calcium cycling in cardiac myocytes: from detailed cleft dynamics to the whole cell concentration profiles. *Front. in Physiol.* 6:590–15.
16. Higazi, D. R., C. J. Fearnley, F. M. Drawnel, A. Talasila, E. M. Corps, O. Ritter, F. McDonald, K. Mikoshiba, M. D. Bootman, and H. L. Roderick, 2009. Endothelin-1-stimulated InsP₃-induced Ca²⁺ release is a nexus for hypertrophic signaling in cardiac myocytes. *Mol. Cell* 33:472–482.
17. Harzheim, D., M. Movassagh, R. S.-Y. Foo, O. Ritter, A. Tashfeen, S. J. Conway, M. D. Bootman, and H. L. Roderick, 2009. Increased InsP₃Rs in the junctional sarcoplasmic reticulum augment Ca²⁺ transients and arrhythmias associated with cardiac hypertrophy. *Proc. Natl. Acad. Sci.* 106:11406–11411.
18. Nakayama, H., I. Bodi, M. Maillet, J. DeSantiago, T. L. Domeier, K. Mikoshiba, J. N. Lorenz, L. A. Blatter, D. M. Bers, and J. D. Molkentin, 2010. The IP₃ Receptor Regulates Cardiac Hypertrophy in Response to Select Stimuli. *Circ. Res.* 107:659–666.
19. Rinne, A., N. Kapur, J. D. Molkentin, S. M. Pogwizd, D. M. Bers, K. Banach, and L. A. Blatter, 2010. Isoform- and tissue-specific regulation of the Ca²⁺-sensitive transcription factor NFAT in cardiac myocytes and heart failure. *Am. J. Physiol. - Heart and Circ. Physiol.* 298:H2001–H2009.
20. Signore, S., A. Sorrentino, J. Ferreira-Martins, R. Kannappan, M. Shafaie, F. D. Ben, K. Isobe, C. Arranto, E. Wybieralska, A. Webster, F. Sanada, B. Ogórek, H. Zheng, X. Liu, F. del Monte, D. A. D'Alessandro, O. Wunimenghe, R. E. Michler, T. Hosoda, P. Goichberg, A. Leri, J. Kajstura, P. Anversa, and M. Rota, 2013. Inositol 1,4,5-Trisphosphate Receptors and Human Left Ventricular Myocytes. *Circulation* 128:1286–1297.
21. Proven, A., H. L. Roderick, S. J. Conway, M. J. Berridge, J. K. Horton, S. J. Capper, and M. D. Bootman, 2006. Inositol 1,4,5-Trisphosphate Supports the Arrhythmogenic Action of Endothelin-1 on Ventricular Cardiac Myocytes. *J. Cell Sci.* 119:3363–3375.
22. Domeier, T. L., A. V. Zima, J. T. Maxwell, S. Huke, G. A. Mignery, and L. A. Blatter, 2008. IP₃ Receptor-Dependent Ca²⁺ Release Modulates Excitation-Contraction Coupling in Rabbit Ventricular Myocytes. *Am. J. Physiol. - Heart and Circ. Physiol.* 294:H596–H604.
23. Ljubojevic, S., S. Radulovic, G. Leitinger, S. Sedej, M. Sacherer, M. Holzer, C. Winkler, E. Pritz, T. Mittler, A. Schmidt, M. Sereinigg, P. Wakula, S. Zissimopoulos, E. Bisping, H. Post, G. Marsche, J. Bossuyt, D. M. Bers, J. Kockskämper, and B. Pieske, 2014. Early Remodeling of Perinuclear Ca²⁺ Stores and Nucleoplasmic Ca²⁺ Signaling During the Development of Hypertrophy and Heart Failure. *Circulation* 130:244–255.
24. Olivares-Florez, S., M. Czolbe, F. Riediger, L. Seidlmayer, T. Williams, P. Nordbeck, J. Strasen, C. Glocker, M. Jansch, P. Eder-Negrin, P. Arias-Loza, M. Mühlfelder, J. Plačkić, K. G. Heinze, J. D. Molkentin, S. Engelhardt, J. Kockskämper, and O. Ritter, 2018. Nuclear Calcineurin Is a Sensor for Detecting Ca²⁺ Release from the Nuclear Envelope via IP₃R. *J. Mol. Med.* .
25. Smyrniak, I., N. Goodwin, D. Wachten, J. Skogestad, J. M. Aronsen, E. L. Robinson, K. Demydenko, A. Segonds-Pichon, D. Oxley, S. Sadayappan, K. Sipido, M. D. Bootman, and H. L. Roderick, 2018. Contractile Responses to Endothelin-1 Are Regulated by PKC Phosphorylation of Cardiac Myosin Binding Protein-C in Rat Ventricular Myocytes. *J. Mol. and Cell. Cardiol.* 117:1–18.
26. Harzheim, D., A. Talasila, M. Movassagh, R. Foo, N. Figg, M. Bootman, and L. Roderick, 2010. Elevated InsP₃R expression underlies enhanced calcium fluxes and spontaneous extra-cystolic calcium release events in hypertrophic cardiac myocytes. *Channels* 4:1–5.
27. Escobar, A. L., C. G. Perez, M. E. Reyes, S. G. Lucero, D. Korniyev, R. Mejía-Alvarez, and J. Ramos-Franco, 2012. Role of inositol 1,4,5-trisphosphate in the regulation of ventricular Ca²⁺ signaling in intact mouse heart. *J. Mol. and Cell. Cardiol.* 53:768–779.
28. Foskett, J. K., C. White, K.-H. Cheung, and D.-O. D. Mak, 2007. Inositol Trisphosphate Receptor Ca²⁺ Release Channels. *Physiol. Rev.* 87:593–658.

29. Ramos-Franco, J., D. Bare, S. Caenepeel, A. Nani, M. Fill, and G. Mignery, 2000. Single-Channel Function of Recombinant Type 2 Inositol 1,4, 5-Trisphosphate Receptor. *Biophys. J.* 79:1388–1399.
30. Siekmann, I., J. Sneyd, and E. J. Crampin, 2014. Statistical analysis of modal gating in ion channels. *Proc. R. Soc. A: Math., Phys. and Eng. Sci.* 470:20140030–20140030.
31. Siekmann, I., P. Cao, J. Sneyd, and E. J. Crampin, 2019. Data-Driven Modelling of the Inositol Trisphosphate Receptor (IP₃R) and its Role in Calcium-Induced Calcium Release (CICR). In M. De Pittà, and H. Berry, editors, Computational Glioscience, Springer International Publishing, Cham, Springer Series in Computational Neuroscience, 39–68.
32. Cao, P., X. Tan, G. Donovan, M. J. Sanderson, and J. Sneyd, 2014. A Deterministic Model Predicts the Properties of Stochastic Calcium Oscillations in Airway Smooth Muscle Cells. *PLoS Comp. Biol.* 10:e1003783–15.
33. Sneyd, J., J. M. Han, L. Wang, J. Chen, X. Yang, A. Tanimura, M. J. Sanderson, V. Kirk, and D. I. Yule, 2017. On the Dynamical Structure of Calcium Oscillations. *Proc. Natl. Acad. Sci.* 114:1456–1461.
34. Siekmann, I., J. Sneyd, and E. J. Crampin, 2012. MCMC can detect nonidentifiable models. *Biophys. J.* 103:2275–2286.
35. Terkildsen, J. R., S. Niederer, E. J. Crampin, P. J. Hunter, and N. P. Smith, 2008. Using Physiome standards to couple cellular functions for rat cardiac excitation-contraction. *Exp. Physiol.* 93:919–929.
36. Wilkins, B. J., L. J. D. Windt, O. F. Bueno, J. C. Braz, B. J. Glascock, T. F. Kimball, and J. D. Molkenin, 2002. Targeted disruption of NFATc3, but not NFATc4, reveals an intrinsic defect in calcineurin-mediated cardiac hypertrophic growth. *Mol. and Cell Biol.* 22:7603–7613.
37. Molkenin, J., J. Lu, C. Antos, B. Markham, J. Richardson, J. Robbins, S. Grant, and E. Olson, 1998. A calcineurin-dependent transcriptional pathway for cardiac hypertrophy. *Cell* 93:215–228.
38. Tomida, T., K. Hirose, A. Takizawa, F. Shibasaki, and M. Iino, 2003. NFAT functions as a working memory of Ca²⁺ signals in decoding Ca²⁺ oscillation. *The EMBO J.* 22:3825–3832.
39. Colella, M., F. Grisan, V. Robert, J. D. Turner, A. P. Thomas, and T. Pozzan, 2008. Ca²⁺ oscillation frequency decoding in cardiac cell hypertrophy: role of calcineurin/NFAT as Ca²⁺ signal integrators. *Proc. Natl. Acad. Sci.* 105:2859–2864.
40. Saucerman, J. J., and D. M. Bers, 2008. Calmodulin Mediates Differential Sensitivity of CaMKII and Calcineurin to Local Ca²⁺ in Cardiac Myocytes. *Biophys. J.* 95:4597–4612.
41. Ulrich, J. D., M.-S. Kim, P. R. Houlihan, L. P. Shutov, D. P. Mohapatra, S. Strack, and Y. M. Usachev, 2012. Distinct Activation Properties of the Nuclear Factor of Activated T-Cells (NFAT) Isoforms NFATc3 and NFATc4 in Neurons. *J. Biol. Chem.* 287:37594–37609.
42. Yissachar, N., T. S. Fischler, A. A. Cohen, S. Reich-Zeliger, D. Russ, E. Shifrut, Z. Porat, and N. Friedman, 2013. Dynamic Response Diversity of NFAT Isoforms in Individual Living Cells. *Mol. Cell* 49:322–330.
43. Kar, P., G. R. Mirams, H. C. Christian, and A. B. Parekh, 2016. Control of NFAT Isoform Activation and NFAT-Dependent Gene Expression through Two Coincident and Spatially Segregated Intracellular Ca²⁺ Signals. *Mol. Cell* 64:746–759.
44. Pandit, S. V., W. R. Giles, and S. S. Demir, 2003. A mathematical model of the electrophysiological alterations in rat ventricular myocytes in type-I diabetes. *Biophys. J.* 84:832–841.
45. Wagner, J., and J. Keizer, 1994. Effects of Rapid Buffers on Ca²⁺ Diffusion and Ca²⁺ Oscillations. *Biophys. J.* 67:447–456.
46. Moschella, M. C., and A. R. Marks, 1993. Inositol 1,4,5-Trisphosphate Receptor Expression in Cardiac Myocytes. *J. Cell Biol.* 120:1137–1146.
47. Siekmann, I., L. E. Wagner II, D. Yule, E. J. Crampin, and J. Sneyd, 2012. A kinetic model for type I and II IP₃R accounting for mode changes. *Biophys. J.* 103:658–668.
48. Ramos-Franco, J., M. Fill, and G. A. Mignery, 1998. Isoform-Specific Function of Single Inositol 1,4,5-Trisphosphate Receptor Channels. *Biophys. J.* 75:834–839.

49. Zima, A. V., E. Bovo, D. M. Bers, and L. A. Blatter, 2010. Ca²⁺ Spark-Dependent and Independent Sarcoplasmic Reticulum Ca²⁺ Leak in Normal and Failing Rabbit Ventricular Myocytes. *J. Physiol.* 588:4743–4757.
50. Blanch i Salvador, J., and M. Egger, 2018. Obstruction of ventricular Ca²⁺-dependent arrhythmogenicity by inositol 1,4,5-trisphosphate-triggered sarcoplasmic reticulum Ca²⁺ release. *J. Physiol.* 596:4323–4340.
51. Cooling, M. T., P. J. Hunter, and E. J. Crampin, 2009. Sensitivity of NFAT cycling to cytosolic calcium concentration: implications for hypertrophic signals in cardiac myocytes. *Biophys. J.* 96:2095–2104.
52. Jansen, M. J. W., 1999. Analysis of Variance Designs for Model Output. *Comput. Phys. Commun.* 117:35–43.
53. Saltelli, A., P. Annoni, I. Azzini, F. Campolongo, M. Ratto, and S. Tarantola, 2010. Variance Based Sensitivity Analysis of Model Output. Design and Estimator for the Total Sensitivity Index. *Comput. Phys. Commun.* 181:259–270.
54. Greenstein, J. L., and R. L. Winslow, 2002. An Integrative Model of the Cardiac Ventricular Myocyte Incorporating Local Control of Ca²⁺ Release. *Biophys. J.* 83:2918–2945.
55. Moravec, C. S., E. E. Reynolds, R. W. Stewart, and M. Bond, 1989. Endothelin Is a Positive Inotropic Agent in Human and Rat Heart in Vitro. *Biochem. and Biophys. Res. Commun.* 159:14–18.
56. Salazar, C., A. Zaccaria Politi, and T. Höfer, 2008. Decoding of Calcium Oscillations by Phosphorylation Cycles: Analytic Results. *Biophys. J.* 94:1203–1215.
57. Dolmetsch, R. E., R. S. Lewis, C. C. Goodnow, and J. I. Healy, 1997. Differential activation of transcription factors induced by Ca²⁺ response amplitude and duration. *Nat.* 386:855–858.
58. Feske, S., R. Draeger, H.-H. Peter, K. Eichmann, and A. Rao, 2000. The Duration of Nuclear Residence of NFAT Determines the Pattern of Cytokine Expression in Human SCID T Cells. *J. Immunol.* 165:297–305.
59. Sparrow, A. J., K. Sievert, S. Patel, Y.-F. Chang, C. N. Broyles, F. A. Brook, H. Watkins, M. A. Geeves, C. S. Redwood, P. Robinson, and M. J. Daniels, 2019. Measurement of Myofilament-Localised Calcium Dynamics in Adult Cardiomyocytes and the Effect of Hypertrophic Cardiomyopathy Mutations. *Circ. Res.* 44:20–24.
60. Gaur, N., and Y. Rudy, 2011. Multiscale Modeling of Calcium Cycling in Cardiac Ventricular Myocyte: Macroscopic Consequences of Microscopic Dyadic Function. *Biophys. J.* 100:2904–2912.
61. Rajagopal, V., G. Bass, C. G. Walker, D. J. Crossman, A. Petzer, A. Hickey, I. Siekmann, M. Hoshijima, M. H. Ellisman, E. J. Crampin, and C. Soeller, 2015. Examination of the effects of heterogeneous organization of RYR clusters, myofibrils and mitochondria on Ca²⁺ release patterns in cardiomyocytes. *PLoS Comput. Biol.* 11:e1004417–31.
62. Ladd, D., A. Tilūnaitė, H. L. Roderick, C. Soeller, E. J. Crampin, and V. Rajagopal, 2019. Assessing Cardiomyocyte Excitation–Contraction Coupling Site Detection From Live Cell Imaging Using a Structurally-Realistic Computational Model of Calcium Release. *Front. in Physiol.* 10:546–15.
63. Mohler, P. J., J.-J. Schott, A. O. Gramolini, K. W. Dilly, S. Guatimosim, W. H. duBell, L.-S. Song, K. Haurogné, F. Kyndt, M. E. Ali, T. B. Rogers, W. J. Lederer, D. Escande, H. L. Marec, and V. Bennett, 2003. Ankyrin-B Mutation Causes Type 4 Long-QT Cardiac Arrhythmia and Sudden Cardiac Death. *Nat.* 421:634–639.
64. Mohler, P. J., J. Q. Davis, and V. Bennett, 2005. Ankyrin-B Coordinates the Na/K ATPase, Na/Ca Exchanger, and InsP₃ Receptor in a Cardiac T-Tubule/SR Microdomain. *PLoS Biol.* 3:e423.
65. Wu, X., T. Zhang, J. Bossuyt, X. Li, T. A. McKinsey, J. R. Dedman, E. N. Olson, J. Chen, J. H. Brown, and D. M. Bers, 2006. Local InsP₃-Dependent Perinuclear Ca²⁺ Signaling in Cardiac Myocyte Excitation-Transcription Coupling. *J. Clin. Investig.* 116:675–682.
66. Cooling, M., P. Hunter, and E. J. Crampin, 2007. Modeling hypertrophic IP₃ transients in the cardiac myocyte. *Biophys. J.* 93:3421–3433.
67. Cooling, M. T., P. J. Hunter, and E. J. Crampin, 2008. Modelling biological modularity with CellML. *Syst. Biol., IET* 2:73–79.

68. Remus, T. P., A. V. Zima, J. Bossuyt, D. J. Bare, J. L. Martin, L. A. Blatter, D. M. Bers, and G. A. Mignery, 2006. Biosensors to Measure Inositol 1,4,5-Trisphosphate Concentration in Living Cells with Spatiotemporal Resolution. *J. Biol. Chem.* 281:608–616.
69. Boivin, B., D. Chevalier, L. R. Villeneuve, É. Rousseau, and B. G. Allen, 2003. Functional Endothelin Receptors Are Present on Nuclei in Cardiac Ventricular Myocytes. *J. Biol. Chem.* 278:29153–29163.
70. Escobar, M., C. Cardenas, K. Colavita, N. B. Petrenko, and C. Franzini-Armstrong, 2011. Structural Evidence for Perinuclear Calcium Microdomains in Cardiac Myocytes. *J. Mol. and Cell. Cardiol.* 50:451–459.
71. Ryall, K. A., D. O. Holland, K. A. Delaney, M. J. Kraeutler, A. J. Parker, and J. J. Saucerman, 2012. Network Reconstruction and Systems Analysis of Cardiac Myocyte Hypertrophy Signaling. *J. Biol. Chem.* 287:42259–42268.
72. Yu, T., C. M. Lloyd, D. P. Nickerson, M. T. Cooling, A. K. Miller, A. Garny, J. R. Terkildsen, J. Lawson, R. D. Britten, P. J. Hunter, and P. M. F. Nielsen, 2011. The Physiome Model Repository 2. *Bioinform.* 27:743–744.
73. Thomas, D., S. C. Tovey, T. J. Collins, M. D. Bootman, M. J. Berridge, and P. Lipp, 2000. A Comparison of Fluorescent Ca²⁺-indicator Properties and Their Use in Measuring Elementary and Global Ca²⁺-signals. *Cell Calcium* 28:213–223.